SENSITIVITY OF THE SYNCHROTRON RADIATION PERTURBED ANGULAR CORRELATION METHOD TO THE ROTATION OF RESONANT MOLECULES

A. Błachowski and K. Ruebenbauer*

Mössbauer Spectroscopy Division, Institute of Physics, Pedagogical University
PL-30-084 Cracow, ul. Podchorążych 2, Poland (sfrueben@cyf-kr.edu.pl)*

The sensitivity of the recently proposed synchrotron radiation perturbed angular correlation (SRPAC) method to the rotation of the molecules containing resonant nuclei has been studied. It was assumed that resonant molecules are embedded in liquids, and that the resonant nuclei experience a hyperfine splitting in the excited state, the latter being generated by the electric field gradient (EFG). The EFG tensor fluctuates by changing the orientation due to the molecular rotation. The case of the first excited state of the ^{57}Fe nucleus embedded in the iron penta-carbonyl molecule has been investigated in some detail. The Monte-Carlo method was used to generate subsequent hyperfine Hamiltonians, and a direct integration of the time dependent Schrödinger equation was used to obtain data patterns. It has been found that SRPAC is sensitive to the above fluctuations for the residence time of the molecule in a particular stochastic state ranging from about 30 ps till almost about 10 μs. A correlation function describing rotations was found to decay very slowly with time passing as $1/\sqrt{1+x}$, where the symbol x denotes a dimensionless reduced correlation time.

Keywords: synchrotron radiation, PAC, liquids, rotation of molecules
PACS Nos: 29.20.Lq, 23.20.En, 61.25.Em, 02.50.Ng

1. Introduction

Perturbed angular correlation (PAC) method is a well-established method to look upon non-scalar hyperfine interactions in the intermediate nuclear state [1,2]. Basically PAC involves three nuclear states, *i.e.*, initial of the highest energy, intermediate, and the final state having the lowest energy. The initial state is usually populated by some decay of the radioactive nucleus. Usually one looks upon time evolution of the angular correlation between two single particles emitted during subsequent decays leading from the initial to the final state, while keeping constant angle between directions of emission of these particles. This arrangement is frequently called time differential PAC – (TDPAC). Hence, the coherence is restricted to a single atom due to the random character of the radioactive decays, and lack of the sufficient energy resolution.

It has been proposed recently to use synchrotron radiation beam of the pulsed character for a similar purpose *i.e.* a new method called synchrotron radiation PAC has been proposed [3,4] nicknamed nowadays as (SRPAC). SRPAC deals with stable resonant nuclei. The initial state is the ground state, the intermediate state is the state resonantly excited by the synchrotron radiation, while the final state is again the ground state upon delayed decay. The origin of time is defined by the prompt pulse from the synchrotron instead of the decay from the initial to the intermediate state. One has to note that the pulse excites many nuclei simultaneously, and hence a nuclear exciton is formed leading to the coherence of the delayed radiation between various emitters [5-7]. One can destroy this coherence using targets having a negligible recoilless fraction, as recently shown in Ref. [8]. Therefore rather broad bandwidth of the incoming radiation has to be applied in order to get sufficient excitation efficiency – in contrast to the arrangement used to look upon phonon density of states (DOS), where a narrow and tunable band has to be used [9]. SRPAC becomes very similar to TDPAC under such circumstances, and hence the coherence is restricted to the excited state of the single resonant atom. Nuclear energy levels involved in PAC and SRPAC are shown in Figure 1.

Therefore, the sensitivity to the translational motions of the resonant atoms is lost, and one can look for the rotational motions alone, as shown recently [10]. In order to do so, one has to count delayed photons emitted at well defined angle between direction of the propagation of that photons and the incoming beam versus time elapsed from the prompt pulse. On the other hand, the excited state has to experience some non-scalar hyperfine interaction of a local character, *i.e.*, generated by a rigid molecule hosting the resonant nucleus. This

interaction has to fluctuate with time passing due to the rotations of the hosting molecule caused by the surrounding dense medium. Hence, the method is likely to be applied to liquids with the above resonant molecules being dissolved within. Such targets are practically unable to absorb reemitted resonant radiation, and thus decay of the delayed radiation is governed by the lifetime of the excited state. Hence, the storage ring has to be operated preferably in a single bunch mode to allow for a complete decay prior to the next pulse. On the other hand, the problem of random coincidences disappears as all excited states are excited simultaneously.

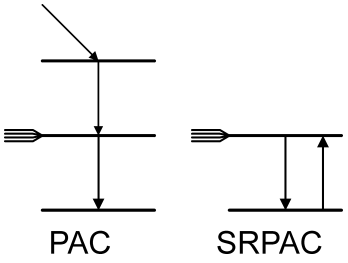

Figure. 1. Nuclear energy levels involved in PAC and SRPAC.

Fluctuating hyperfine interactions are usually treated within the super-operator formalism [11-14]. However, this formalism requires a rather well defined number of stochastic states in order to be efficient. One cannot expect sharply defined stochastic states in the liquid, and hence a different approach is necessary to calculate SRPAC patterns originating from such targets. There are several more or less successful approaches to the continuum of the stochastic states within the super-operator formalism, but they are restricted to the very special cases [13,14].

SRPAC method is neither sensitive to the wave numbers of the incoming and outgoing radiation nor to the wave number transfers to the system investigated. Hence, it is similar to the nuclear quadrupole resonance (NQR) method. However, NQR is sensitive to the much slower fluctuations than SRPAC.

The paper is organized as follows: section 2 is devoted to the general formalism applicable to the cases with a quasi-infinite number of the stochastic states, section 3 discusses plausible non-scalar Hamiltonians present in liquids, while section 4 is concentrated on the choice of the suitable hosting molecules. Numerical results are shown in section 5, while the last section 6 is devoted to the discussion of results and conclusions.

2. General formalism

A typical experimental setup for SRPAC measurements is shown in Figure 2. Usually one has to avoid forward scattered radiation, and hence the scattering angle has to be greater than zero. One can count either delayed photons due to the radiative decay of the excited resonant nuclear state or internal conversion electrons resulting from the decay of the above nuclear state. Eventually some secondary radiation following internal conversion could be detected instead. However, photons following radiative decay have the biggest energy of all the delayed particles emitted. Hence, they are the most penetrating radiation as long as the non-resonant electronic absorption is considered. Therefore it seems wise to rely upon these photons even for high total internal conversion coefficients. Electrons are likely to be multiple scattered prior to leaving sample, and hence they seem useless. This section is devoted to the description of the basic formalism applicable.

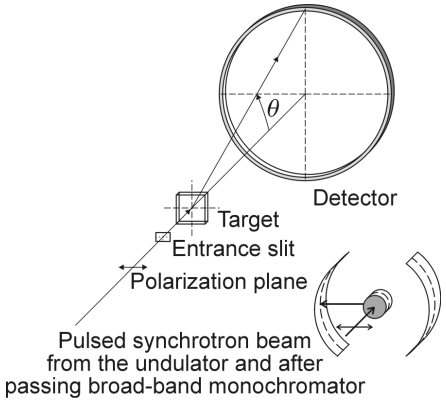

Figure. 2. Basic experimental setup shown in a schematic way. Inset shows the best geometry for dipolar transitions (*e.g.* M1 transition to the first excited state of $^{57}\mathrm{Fe}$) with scattering angle being close to the right angle.

One obtains the following expression for the observable radiation intensity provided SRPAC patterns are recorded for a single photon excitation from the stable ground nuclear level to some meta-stable excited nuclear level followed by a single photon de-excitation back to the ground nuclear state:

$$I(t,\theta) = S_0 \exp[-(t/\tau_N)]\, B(t,\theta)\,. \qquad (1)$$

Here the symbol $S_0 > 0$ stands for the scaling factor, $t \geq 0$ denotes time elapsed from the instant of the nuclear excitation, while $\tau_N > 0$ stands for the average lifetime of the excited nuclear state, the latter being practically independent on the environment of the nucleus. The above expression applies to a linear detector with the negligible background. A perturbation function $B(t,\theta)$ depends upon the scattering angle $0 \leq \theta < \pi$ between incoming and outgoing photons, and it takes on the following form:

$$B(t,\theta)=\sum_{m_e\mu_e} a(m_e\mu_e \mid \theta)\left(\sum_{m_e'\mu_e'} < m_e \mid \exp[-i\int_0^t dt' \mathbf{H}_e(t')] \mid m_e' > < \mu_e' \mid \exp[i\int_0^t dt' \mathbf{H}_e^{+}(t')] \mid \mu_e > \right). \qquad (2)$$

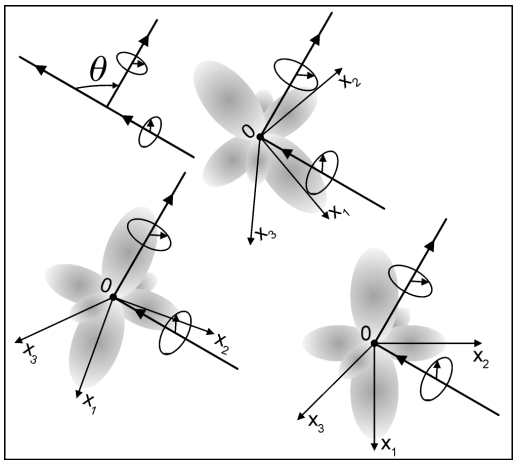

Figure 3. Random orientation of the quantization coordinates in the frame defined by incoming and outgoing photons

The last expression applies to the cases with thermally equalized ground nuclear state hyperfine sublevels, and for the cases with the negligible probabilities of the direct transitions between various excited nuclear state hyperfine sublevels during the lifetime of the excited state. It is further assumed that the detector is insensitive to the polarization of the incoming radiation, and that the sample has completely random orientation as shown in Figure 3. It is assumed that the excited nuclear state hyperfine Hamiltonian $\mathbf{H}_e(t')$ has semi-classical character, and that the hyperfine interaction in this state is non-scalar. The indices m_e and μ_e denote magnetic quantum states of the excited nuclear state e.

Coefficients $a(m_e\mu_e \mid \theta)$ can be calculated in a straightforward manner for a particular nuclear transition applying standard PAC formalism [1,2,15]. The hyperfine Hamiltonian involved is generally time dependent due to the fluctuations of the hyperfine interactions despite the sample as a whole remains at equilibrium. The symbol $(...)$ denotes here the average over the ensemble. It is practical to normalize the coefficients $a(m_e\mu_e \mid \theta)$ in such a way to have $B(t=0,\theta)=1$.

One has to note that the observed signal is further averaged over the time interval of the particular data channel. Usually all these intervals are equal to each other. The signal is inaccessible at very short times elapsed since the prompt pulse as the detector has to recover after the prompt.

The above formalism applies to the resonantly thin target scattering into incoherent channel. Hence, it is desirable for the recoilless fraction to be negligible. In such case it is important to have bandwidth of the incoming exciting radiation encompassing completely phonon bandwidth and eventual bandwidth of the mode coupling theory β-process [16,17]. Such bandwidth of the incident radiation is still monochromatic from the point of view of the detector. It is assumed here as well that the delayed radiation disappears completely prior to the next prompt pulse. The origin of time occurs at prompt on the detector. Here it is assumed that the detector counts directly delayed photons re-emitted from the excited resonant nuclei, and that radiation of different kind can be neglected.

The most general and successful formalism devised up to now to deal with the fluctuating hyperfine interactions is the super-operator formalism [11-14]. The above mentioned ensemble is replaced by the super-operator consisting of the relaxation matrix and a super-Hamiltonian. The dimension of the resulting Hilbert space equals $N(2I_e+1)^2$, where the symbol I_e denotes the spin of the excited nuclear level, while the symbol N denotes the number of stochastic states involved. For a rotating molecule in the dense liquid the number of stochastic states is quasi-infinite, and hence the super-operator formalism fails to be effective. Hence, one has to resort to the direct integration over time and over the ensemble. In such case it is impossible to split perturbation function into “hard core” and time dependent components, as one cannot define diagonal base in the Hilbert space. The only exception is the Hamiltonian commuting with itself at different times. Hamiltonians having this property cannot be used in the case of rotating frames. There are several approaches to the above problem within the super-operator formalism [13,14], but one has to be careful while applying them as they are restricted to the very special cases.

3. Stochastic Hamiltonian

It is obvious that magnetic dipole and quadrupolar electric interactions are the sole non-scalar hyperfine interactions sufficiently strong to be able to split nuclear levels on the time scale accessible to the SRPAC method. A magnetic dipole interaction is likely to be completely averaged out in the liquid state (if present). Hence, one is left with the quadrupolar electric interaction. In order to proceed further some additional assumptions are necessary. It is assumed that the resonant nuclei are embedded in the identical molecules

with single nucleus per molecule. All of them experience the same electric field gradient (EFG) in the principal coordinates of the molecule. On the other hand, the above molecules are dissolved randomly in a solvent free of the resonant nuclei in such a way, that the interactions between molecules containing resonant nuclei can be neglected. It is assumed that neither temperature nor the interaction with the solvent has influence on the EFG in the local principal coordinates. On the other hand, resonant molecules experience random jumps of the very short duration due to the interaction with the dense solvent, and remain in the stationary states between jumps. Hence, the rotational spectra of the resonant molecules are completely smeared out. Due to the fact, that SRPAC is sensitive to the rotational component of the resonant molecule motion solely [18] one can make the following simple model provided the resonant molecule behaves like a rigid body. One can choose principal coordinates of the given molecule under consideration as the quantization coordinates. Hence, one obtains the following interaction tensor at prompt [19]:

$$\mathbf{A} = A_Q \begin{bmatrix} \eta - 1 & 0 & 0 \\ 0 & -(\eta + 1) & 0 \\ 0 & 0 & 2 \end{bmatrix}. \qquad (3)$$

Here the symbol $A_Q = \left(\frac{\mathrm{e} Q_e V_{33}}{4 I_e (2 I_e - 1) \hbar} \right)$ stands for the coupling constant with the symbol e standing for a positive elementary charge, Q_e being spectroscopic nuclear quadrupole moment in the excited state (point-like), V_{33} standing for the third principal component of the EFG on the point-like nucleus, and $\hbar$ being the Planck's constant divided by 2π. One has to note that the excited state nuclear spin has to satisfy the condition $I_e \geq 1$ in order to get splitting. A coupling constant has to be non-zero to get splitting as well. The asymmetry parameter is defined as $\eta = (V_{11} - V_{22})/V_{33}$. It satisfies the following condition $0 \leq \eta \leq 1$ provided $|V_{11}| \leq |V_{22}| \leq |V_{33}|$ with V_{11} and V_{22} being the remaining principal components of the EFG. The asymmetry parameter equals zero for molecules having at least single triple axis passing through the resonant nucleus. The corresponding hyperfine Hamiltonian takes on the following rotationally invariant form [19]:

$$\mathbf{H}_e = \sum_{jk=1}^{3} A_{jk} \, \mathbf{I}_j^{(e)} \, \mathbf{I}_k^{(e)} . \qquad (4)$$

Here the symbols A_{jk} denote Cartesian components of the tensor $\mathbf{A}$, while the operators $\mathbf{I}_j^{(e)}$ and $\mathbf{I}_k^{(e)}$ stand for the nuclear spin projection operators on the respective right-handed Cartesian axes – in the nuclear state e.

Rotational jumps transform the EFG, and hence the tensor $\mathbf{A}$ in the following way: $\mathbf{A} \Rightarrow \mathbf{R}(\alpha\beta\gamma)^{-1} \, \mathbf{A} \, \mathbf{R}(\alpha\beta\gamma)$ at each jump. Here the symbol $\mathbf{R}(\alpha\beta\gamma)$ denotes the Eulerian rotation operator with γ being azimuthal angle, β denoting polar angle, and α standing for the third Eulerian angle. The rotation by the third Eulerian angle can be dropped for the axially symmetric EFG. Hence, each rotation generates a new hyperfine Hamiltonian according to the equation (4), and the hyperfine Hamiltonian becomes time dependent. One has to note that all these subsequent Hamiltonians have the same set of eigenvalues. It is assumed that subsequent jumps remain uncorrelated each other. Subsequent rotations apply to the tensor $\mathbf{A}$ resulting from the previous rotation except the first rotation acting on the tensor described by the equation (3).

In order to proceed further one has to introduce distributions of the Eulerian angles at jump. In principle such distributions can be calculated within the framework of the molecular dynamics (MD) [16,17] provided interactions between solvent molecules and between solvent and resonant molecules are known. Otherwise, one has to resort to some simple approximations. Due to the fact that SRPAC (and other methods as well) are not particularly sensitive to the details of the stochastic jumps provided the latter occur within quasi-infinite set of the states, there is little hope to get sufficiently precise data to perform realistic MD calculations. It is assumed here that all points on the unit sphere are equally accessible during the jump, and the same assumption is made for the third Eulerian angle. Hence, one obtains:

$$\alpha = 2\pi \, R_n \, , \; \beta = \mathrm{a}\cos(1 - 2R_{n+1}) \quad \text{and} \quad \gamma = 2\pi \, R_{n+2} \, . \qquad (5)$$

Here the symbols $0 < R_n < 1$ denote subsequent pseudo-random numbers having flat distribution within the range $(0,1)$. The index n increases by unity after each generation of such number. It is assigned value $n = 0$ at the beginning of the series.

The residence time between jumps has random duration as well. A distribution of these times has to follow from the MD calculations as well. However, as long as the above mentioned interactions remain unknown one has to apply some simple approximation again. There is an implicit assumption within the framework of the formalism of the stochastic operators [13,14] that such a distribution is exponential for each stochastic state. Hence, it is assumed that the system exhibits no memory of the past. Here one has more freedom of choice. It is assumed here that this distribution is Poissonian-like taking on the form:

$$\rho(x) = x e^{-x} . \qquad (6)$$

If one denotes by the symbol $\Delta t = (x\tau)/ < x >$ subsequent residence time with $\tau > 0$ being the average residence time, and $< x >= \int_0^\infty dx\, x\, \rho(x)$ being the average of the distribution $\rho(x)$, one has to obtain the corresponding value of the variable x. It has to be noted that the distribution given by the equation (6) satisfies two general conditions for $x \geq 0$, *i.e.*, $\rho(x) > 0$ (except $\rho(0) = 0$) and $\int_0^\infty dx\, \rho(x) = 1$. For this particular distribution the average $< x >= 2$. Hence, one has to solve the following equation in order to obtain particular residence time after jump:

$$R_{n+3} = \int_0^x dx'\, \rho(x'). \qquad (7)$$

Once a particular value for the variable x is obtained one can calculate Δt as $\Delta t = \frac{1}{2} x\tau$. Hence, the dynamics depends upon the single parameter τ within this simple above outlined model.

Additionally, at the beginning of each independent history one has to choose time of the first jump after prompt. If one has calculated a particular residence time after jump nearest to the prompt and in the past of the prompt one can calculate this time as $t_0 = (1 - R_{n+4})\Delta t$, where Δt refers here to this particular residence time. Each history has to be continued past the time window of the detector. Pseudo-random numbers used in all histories have to belong to the same series. All histories are equivalent within this model.

The above simple model of rotations basically depends upon single parameter τ, the latter parameter being the average residence time. For very large residence time one obtains a static pattern, while for the residence time going to zero the observed hyperfine interactions are averaged to some kind of the asymptotic form, *i.e.*, some kind of the motional narrowing is obtained.

The above formalism seems more general than the formalism of the stochastic operators as it allows to deal with quasi-infinite number of the stochastic states and gives more freedom upon the choice of the distribution of the residence times. Usually in a crystalline state one has well defined number of the stochastic states. On the other hand, the number of such states is very large and poorly defined in the liquid. The model outlined above is basically a strong collision model [13] tractable in principle within the super-operator formalism. However a direct integration method allows for the unrestricted extensions of the stochastic models particularly in the form outlined above. A strong collision model seems satisfactory for the low and intermediate viscosity liquids or for the high viscosity liquids hosting small resonant molecules, the latter fitting well into spheres.

4. Choice of the resonant molecules

The best resonant line at the present state of the art seems to be the single photon line connecting ground level of the stable ^{57}Fe isotope with the first excited level of this isotope having energy $14.41\,\mathrm{keV}$ above the ground state. The ground state has nuclear spin $I_g = \frac{1}{2}^{(-)}$, while the first excited nuclear state has spin $I_e = \frac{3}{2}^{(-)}$. A single photon transition is practically of the pure M1 character, and hence a contribution resulting from the E2 amplitude is negligible. The abundance of this resonant isotope is about 2.19 at. % in natural iron allowing for various distinctly different enrichment ratios. The first excited state has a lifetime τ_N close to 141.1 ns. Some inconvenience is caused by the relatively high total conversion coefficient of this transition [19]. Hence, the ground state remains as a singlet under action of the EFG, while the excited state splits into pair of Kramers doublets without shift of the average energy. Therefore one sees single hyperfine energy represented by the splitting of the excited state [20].

On the other hand, it seems that iron penta-carbonyl $Fe(CO)_5$ might be suitable resonant molecule [21]. It contains single resonant atom per molecule in the rather well defined environment. Bonds between iron and adjacent carbons belonging to the CO groups are highly covalent. Hence, the EFG generated splitting practically depends neither upon temperature nor surrounding of the molecule [22]. Electronic magnetic moment of the molecule is null assuring absence of the hyperfine magnetic splitting without applying external magnetic field [21]. Molecules are rather small and highly symmetric. They form slightly distorted bi-pyramids of the almost regular triangular base as shown in Figure 4, and they are non-polar molecules. Dimension along the polar axis is almost the same as the diameter in the equatorial plane [21].

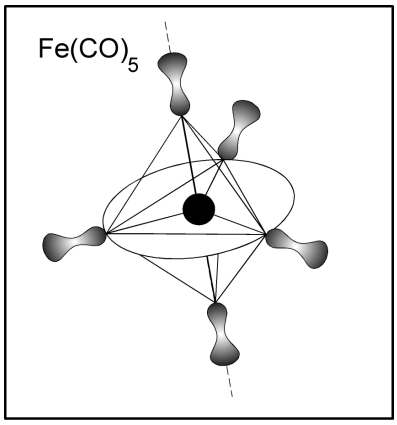

Figure 4. Iron penta-carbonyl molecule having *D3h* symmetry. Distance between centers of the outermost oxygens along the triple axis is about 0.584 nm.

One can expect for the asymmetry parameter to be almost zero, *i.e.*, one can expect that the condition $\eta = 0$ is reasonably satisfied, as the triple axis is present in the bi-pyramid structure above mentioned [21]. Hence, the coupling constant can be obtained as $|A_Q| = \frac{1}{6}\Delta_Q$, where $\Delta_Q > 0$ stands for the splitting of the excited state. Here experimental data remain insensitive to the sign of the coupling constant, and thus one can use the effective coupling constant defined as $A_Q^{(eff)} = \frac{1}{6}\Delta_Q$. However, the sign of the coupling constant was found as being positive by means of the Mössbauer spectroscopy, and the coupling constant was determined as $A_Q = +0.0309\ \mathrm{ns}^{-1}$ [23].

Iron penta-carbonyl remains liquid under normal pressure in the approximate temperature range 253 – 376 K. It has density of about 1.5 $\mathrm{g/cm}^3$ in the vicinity of the room temperature under normal pressure and for the natural isotopic composition. It is insoluble in the polar solvents, but it dissolves easily in a variety of non-polar iron-free organic solvents without decomposition. Molecules start to decompose in the gaseous phase above the approximate temperature of 470 K. Hence they remain intact in either pure liquid phase or in the solutions. A decomposition of the molecules might start at lower temperatures after having embedded them into strongly interacting host. A partial decomposition was observed above about 370 K in some zeolites [24]. Some decomposition or transition to carbonyls containing multiple iron atoms (the latter phenomenon occurs for densely packed molecules) appears due to photo-dissociation, but this phenomenon should be minor problem, as many more fragile organic compounds survive exposition to the synchrotron radiation. Spatial in-coherency in pure liquid can be assured by the partial enrichment of the sample in the resonant isotope. Measurements have to be performed for well defined composition of the liquid sample, and at constant hydrostatic pressure varying temperature between subsequent runs, as the sole dynamic parameter τ depends upon temperature, sample composition, and to a lesser extend on the pressure.

5. Numerical simulations

Numerical simulations were performed for the following set of parameters:

$$\theta = 90^{\mathrm{o}},\ \tau_N = 141.1\ \mathrm{ns},\ A_Q = +0.0309\ \mathrm{ns}^{-1},$$
$$\eta = 0,\ S_0 = 10^4 \text{ and } \tau_D = 5.1\ \mathrm{ns}.$$

Here $\tau_D > 0$ denotes dead time of the detector after the prompt pulse. A time window of the detector was divided into 512 channels having 1 ns width each of them. This window starts at the prompt pulse. Three equally spaced data points were calculated for each of the above channels, *i.e.*, a time resolution was kept to within 1/3 ns during all simulations. A parameter τ was varied, of course. The numerical data are averaged over 10^3 independent histories in each case except the shortest residence times, where 100 histories were used for $\tau = 1$ ps, and 10 histories for $\tau = 0.1$ ps. Hence, the "experimental" time window used in the present simulations extends from 6 ns till 512 ns. It has to be noted that in order to avoid counts from the previous pulse one needs a separation between pulses of the order of 1.5 μs at least. Fortunately, currently available storage rings are able to provide such long time intervals between pulses provided they are operated in the single bunch mode. These long time scales are due to the lack of the formation of the nuclear exciton, and hence to the lack of speedup.

Calculated intensities $I(t,\theta)$ have been additionally transformed within the "experimental" time window into intensities $I_E(t,\theta)$ applying standard random statistical scatter in order to simulate more realistically experimental data. Similarly one can calculate the "experimental" function

$$B_E(t,\theta) = I_E(t,\theta)/\{S_0 \exp[-(t/\tau_N)]\},$$

the latter function being a good measure of the experimental sensitivity. In order to introduce above data scatter a Gaussian shape random number generator was used with dispersion depending on the actual value of the function processed. Simulated patterns are shown in Figures 5 - 7. The total number of counts "accumulated" within the detector time window varied from about 1.50×10^6 counts till about 2.69×10^6 counts depending upon the residence time. The maximum occurs at residence times being close to 10 ns. One has to note that the same scaling factor was used in all simulations.

The range of the scattering angles encompassed by the detector has to be small enough to allow for the approximation by the average scattering angle, and in order to prevent excessive smoothing of the data patterns on the time scale. One can use two detectors simultaneously as the same patterns occur at the scattering angle θ and $\pi - \theta$. However, the best choice is to use a single detector with the scattering angle being close to the right angle.

One can expect about 100 counts per second on the detector provided the sample has optimized thickness, and the storage ring is tuned well. Hence, the data set of the sufficient quality can be accumulated within about several hours.

In the case of rapidly fluctuating hyperfine Hamiltonian described by the expression (4) one can define the average Hamiltonian as:

$$\mathbf{H}_e(n) = \frac{1}{n}\sum_{m=1}^{n}\mathbf{H}_e(m). \qquad (8)$$

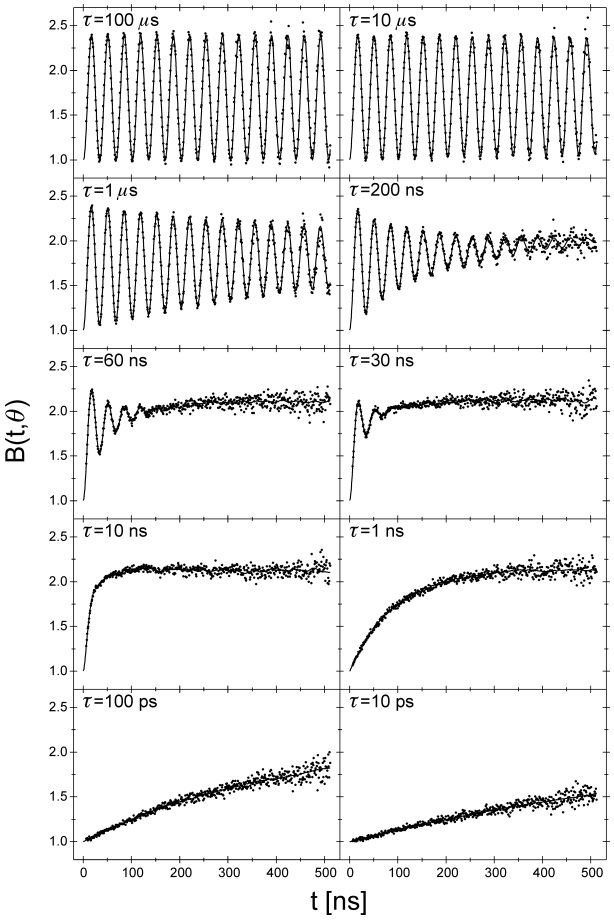

Figure 5. Function $B(t,\theta)$ plotted versus time for various residence times. Dots represent corresponding function $B_E(t,\theta)$.

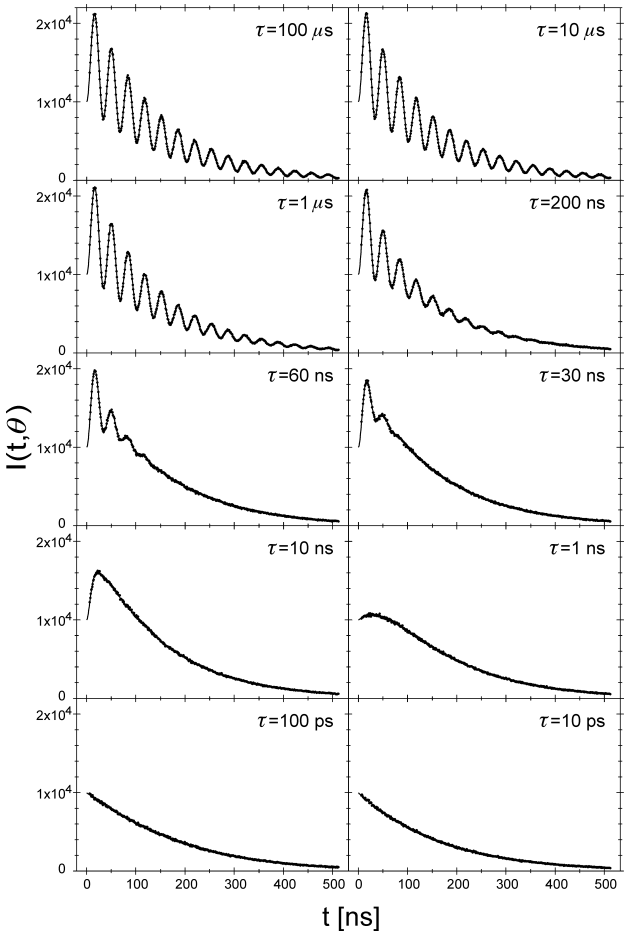

Figure 6. Expected signal $I(t,\theta)$ plotted versus time for various residence times. Dots represent corresponding function $I_E(t,\theta)$.

Here the index $n = 1, 2, \ldots$ denotes the number of stochastic states visited since the origin of the time scale, *i.e.*, since the occurrence of the prompt pulse. One can calculate splitting $\Delta_Q(n)$ caused by such Hamiltonian for the nuclear spin taking on the value $I_e = \frac{3}{2}$. Hence, it is possible to define the following function of the above index: $\varepsilon(n) = \Delta_Q(n)/\Delta_Q(n=1)$. If one plots $-\ln[\varepsilon(n)]$ versus $\ln(n)$ one obtains a straight line going through the origin. Figure 8 shows such plots averaged over 100 independent series, and calculated for the asymmetry parameter taking on the values 0, 0.5 and 1.

Due to the fact that the time scale for long series is approximated quite well by the expression

$$t = (n-1)\tau$$

one can conclude that the function $\varepsilon(t)$ satisfies the following equation:

$$\varepsilon(t) = \left(\frac{\tau}{\tau + t}\right)^c . \qquad (9)$$

Here the symbol c denotes the slope of the above straight line shown in Figure 8, where the values obtained for the slope are indicated as well. One can conclude that the slope is practically independent of the asymmetry parameter and it approximates quite well to the value $c = \frac{1}{2}$. Hence, the function $\varepsilon(t)$ reduces to the following very simple form: $\varepsilon(t) = [\tau/(\tau + t)]^{1/2}$. For a dimensionless reduced time $x = t/\tau$ one obtains $\varepsilon(x) = 1/\sqrt{1+x}$.

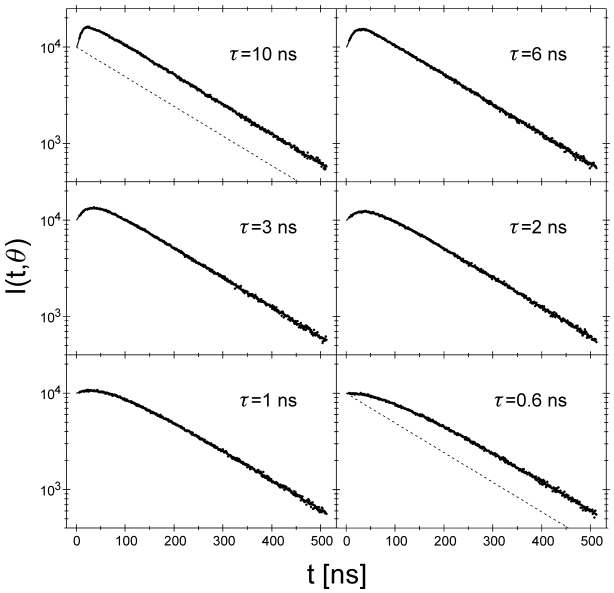

Figure 7. Signal $I(t,\theta)$ plotted on the logarithmic scale versus time and for various residence times. Dashed lines show simple exponential decay in the absence of the hyperfine interactions with the same scaling factor as applied to the original data. Dots represent corresponding function $I_E(t,\theta)$.

It is interesting to observe that the average splitting diminishes very slowly with time passing. This behavior is due to the fact, that neither the coupling constant nor the asymmetry parameter depends on time. On the other hand, there is a quasi-continuum of the stochastic states available. One can treat the equation (9) as a definition of the self-correlation function. This function is obviously non-exponential in similarity to the Kohlrausch function [25], and it decays even more slowly than the Kohlrausch function for large values of time. It can be defined for a single particle, and hence its peculiar behavior has nothing to do with the averaging over the ensemble. This function obeys the following differential equation:

$$\partial\varepsilon/\partial t = -\left(\frac{c}{\tau+t}\right)\varepsilon(t). \tag{10}$$

The above behavior of the self-correlation function has enormous effect on the phase operators of the expression (2). Namely, one can approximate the phase operator by the following expression in the case of very rapid fluctuations:

$$\begin{aligned} &\mathbf{\Psi}(x) = \int_0^x dx' \,\mathbf{H}_e(x') \approx <\mathbf{H}_e(x)> x \\ &\text{with } <\mathbf{H}_e(x)> = x^{-1}\int_0^x dx' \,\mathbf{H}_e(x'). \end{aligned} \tag{11}$$

On the other hand, the average Hamiltonian takes on the following form applying the self-correlation function obtained above:

$$<\mathbf{H}_e(x)> = \mathbf{H}_e(0)\,(1+x)^{-1/2}. \tag{12}$$

Hence, one obtains finally the following expression for the approximate phase operator:

$$\mathbf{\Psi}(x) = \mathbf{H}_e(0)\left(\frac{x}{\sqrt{1+x}}\right). \tag{13}$$

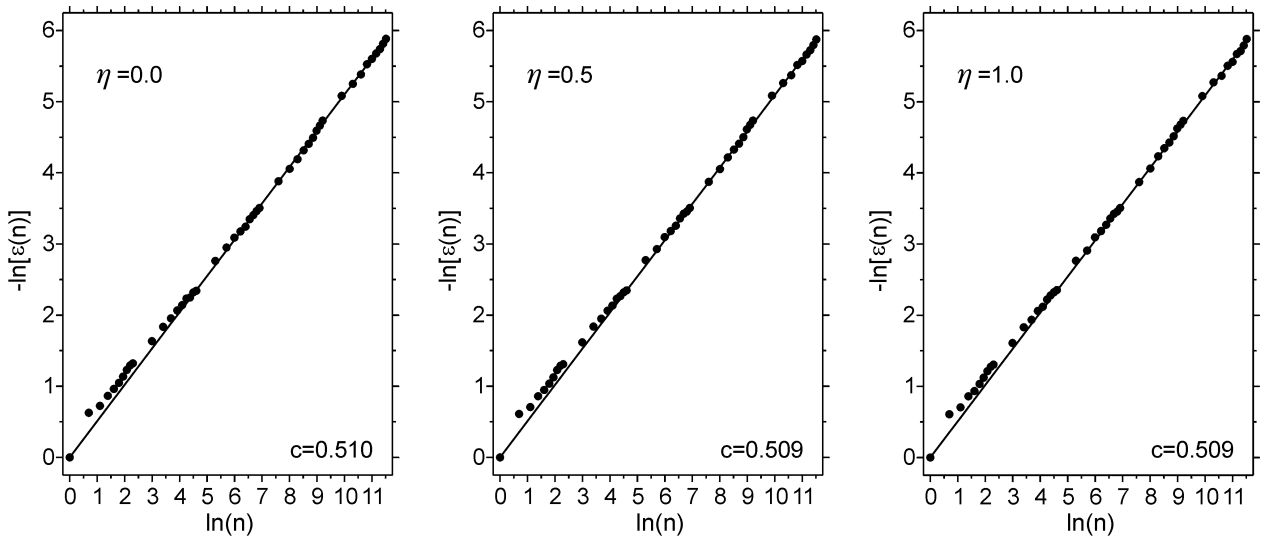

Figure. 8. Plots used to determine exponents of the self-correlation functions.

It is interesting to note, that the above phase operator does not average out with the increasing reduced time x. In order to do so, it is necessary for the correlation function to decay faster than $1/x$ for large values of x. Therefore rigid rotations alone are unable to remove completely imprint of the hyperfine interactions on the data even in the very fast fluctuation limit. Such removal is accomplished by the rotating molecule deformation occurring at much higher temperatures. These effects are not taken into account here as it is assumed that the resonant molecules survive intact till the boiling point.

For very short residence times τ the TDPAC arrangement fails to be sensitive to the fluctuations. However it is still possible to extract some information applying time integral PAC (TIPAC) approach to the data. This approach is similar to the recently proposed procedure to observe fast diffusion in the resonant coherent forward scattering by means of the interferometric method [26,27]. First of all, it is assumed here that the time interval per data channel is much shorter than the characteristic time scale due to the static hyperfine interaction $(2\pi)/\Delta_Q$. In such case one can define the following ratio:

$$R(\tau)=\left(\int_{t_1}^{t_2} dt\, I(t,\theta)\right)\Big/\left(S_0\int_{t_1}^{t_2} dt\,\exp[-(t/\tau_N)]\right). \quad (14)$$

Here the symbols t_1 and t_2 denote lower and upper borders of the detector time window, respectively, and they satisfy the following condition $0<t_1<t_2$. The above ratio is an implicit function of the parameter τ via the intensity $I(t,\theta)$. The model outlined here allows for calculating this ratio, however in the real experimental situation the scaling factor S_0 has to be treated as the adjustable parameter together with the parameter τ. The above ratio is shown versus residence time in Figure 9. The error of the ratio was obtained simulating the same data patterns with various initial values of the pseudo-random numbers generator seed.

Hence, in order to use the ratio defined by the expression (14) one has to estimate the scaling factor as accurately as possible. The most difficult region extends between approximately 10 ns and 1 ns, where it is required to have small delay times τ_D in order to estimate correctly slope of the data pattern at early times. The problem becomes less serious for shorter residence times, particularly in the extreme saturation region.

For residence times shorter than about 10 ns, and for sufficiently early times after the prompt pulse, one can apply a linear regression of the following form in order to estimate the required scaling factor:

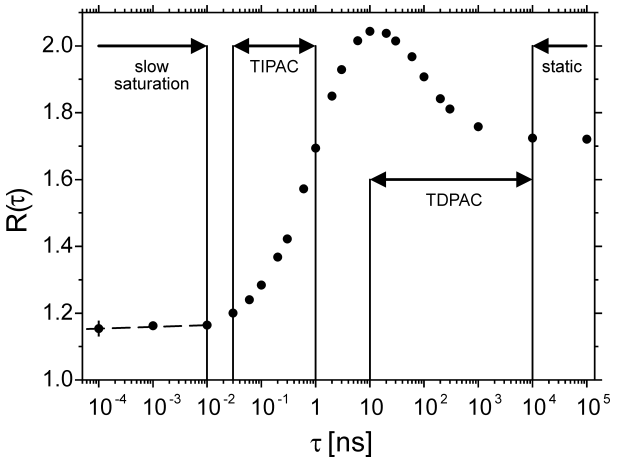

Figure 9. Ratio $R(\tau)$ plotted versus residence time. Particular regions of sensitivity to the fluctuations are indicated approximately.

$$\ln[I(t,\theta)]=\ln(S_0)-t\left[(1/\tau_N)-\left(\frac{\partial B}{\partial t}\right)_{t=0}\right]. \quad (15)$$

There are not very many suitable data points to perform this fit to the two parameters in the vicinity of the residence time approaching about 1 ns, and hence this region is likely to produce large errors. Several values of the slope $\left(\frac{\partial B}{\partial t}\right)_{t=0}$ are listed for various residence times τ in Table 1. These values can be used to estimate the experimental residence time provided the EFG parameters are close to those of iron penta-carbonyl, scattering angle is close to the right angle, and the residence time falls within the range 10 ns till down 0.6 ns. Errors listed in Table 1 are differences between two independent simulations starting at different seeds of the random number series.

Table 1

Parameters $\left(\frac{\partial B}{\partial t}\right)_{t=0}$ listed for various residence times τ. The parameters were obtained fitting the function $B(t,\theta)$ to the straight line for time t lesser than $20\,\text{ns}$.

τ [ns]	$\left(\frac{\partial B}{\partial t}\right)_{t=0}$ [ns^{-1}]
10	0.048991 ± 0.001809
6	0.038359 ± 0.000098
3	0.025641 ± 0.000017
2	0.019085 ± 0.001013
1	0.010873 ± 0.000795
0.6	0.007351 ± 0.000905

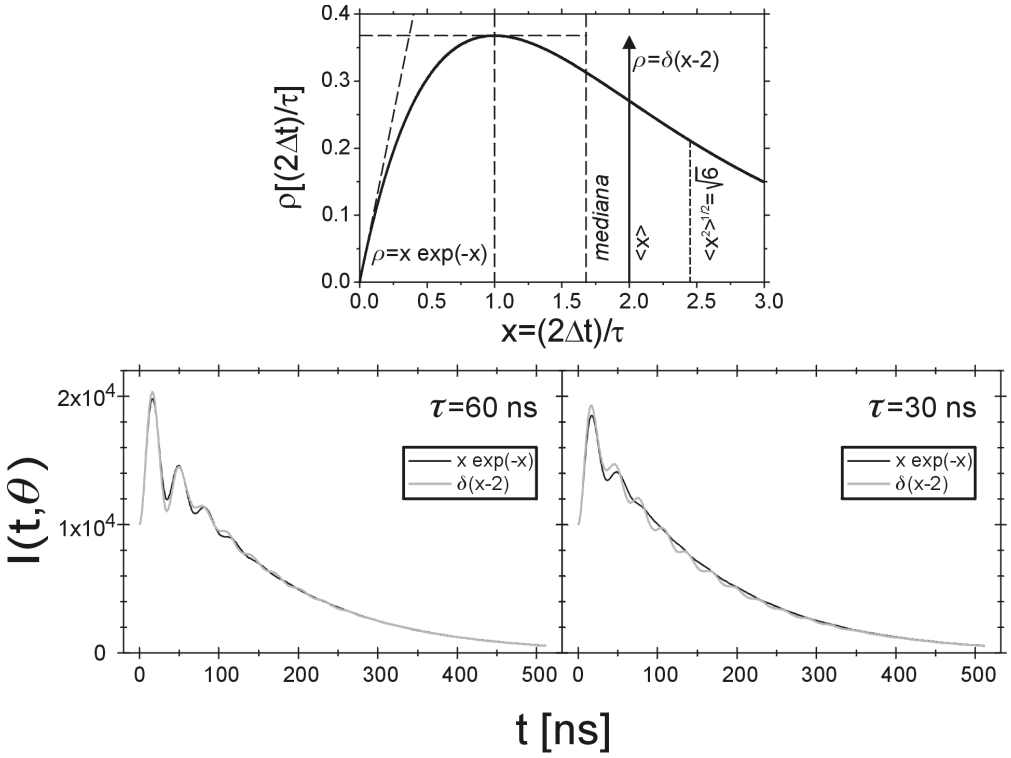

Figure 10. Comparison of the Dirac-delta data patterns with the patterns simulated using equation (6). Upper part shows respective distributions of the residence time.

In order to answer the question about the data sensitivity to the shape of the residence time distribution some data patterns $I(t,\theta)$ were simulated applying Dirac-delta distribution $\delta(x-2)$ instead of the distribution described by the equation (6). All parameters were kept at the same values as used for the corresponding simulations with the equation (6). One has to realize that the last model is highly unrealistic, as it implies that all molecules behave in a clock-like manner maintaining the same residence time for all events involved. Results are plotted in Figure 10. It has been found that signals differ insignificantly for residence times either shorter than about 30 ns or longer than about 60 ns. Hence, the highest sensitivity is achieved for residence times being comparable to the inverse quadrupolar frequency. Functions $B(t,\theta)$ still differ for somewhat longer residence times, albeit for so long times elapsed from the prompt, that these regions are practically inaccessible experimentally. One can practically reproduce all Dirac-delta patterns by the equation (6) patterns adjusting the average residence time in the latter case.

One has to note that the parameter $< x^2 >^{1/2}$ of Figure 10 follows from the equation:

$$< x^2 >^{1/2} = \sqrt{\int_0^\infty dx\, x^3 \exp(-x)}\,. \qquad (16)$$

The parameter called *mediana* is a solution of the following equation:

$$\int_0^{mediana} dx\, x \exp(-x) = \tfrac{1}{2}\,. \qquad (17)$$

6. Discussion and conclusions

It seems that SRPAC might be suitable method to look upon rotations of molecules in liquids. It might fill a gap between NQR and microwave spectroscopy time windows. In order to be successful it is essential to find a proper molecule containing resonant nucleus. Proper molecule has to generate EFG splitting of the sufficient strength in the excited nuclear state studied. A coupling constant and the asymmetry parameter should be insensitive to the local surrounding of the probing molecule. It seems that iron penta-carbonyl molecules are good candidates. On the other hand, the first excited state of the ^{57}Fe nucleus is the best nuclear level for the purpose in the present state of the art. Rotations have influence on the data provided the residence time ranges approximately between 30 ps and almost 10 μs .

One can observe that the correlation function describing rotations of the molecules in liquids via the EFG fluctuations decays very slowly. Hence, it has some resemblance to the Kohlrausch function describing

translations in liquids or glasses [25]. One has to note that the stochastic operator method generates a correlation function as a combination of exponential functions versus time. On the other hand, systems exhibiting a quasi-continuum of stochastic states exhibit much more slowly decaying correlation functions. The model outlined here produces this type of correlation function.

Due to the fact, that the dimensionality of the Hilbert space encompassing all quantum and stochastic states is ill-defined and very large, one has to rely on the direct integration of the Schrödinger equation with the time dependent hyperfine Hamiltonian. The Monte-Carlo method seems to be the best way to generate subsequent hyperfine Hamiltonians. The latter method relies upon few parameters as compared to other methods, and it is easy to include results obtained independently either in the experimental way or due to calculations *e.g.* applying MD method, if possible. Therefore strong collision or rotational diffusion models treated in the isotropic approximation and within the super-operator formalism [13] seem an approximation to the reality. Actually they might be good approximation provided a time window of the particular method is rather narrow. It has to be stressed that direct integration has to be performed on the complete $B(t,\theta)$ function as otherwise results are similar to the results obtained for the above mentioned approximate models [13].

The exact shape of the residence time distribution seems irrelevant, as SRPAC data patterns are rather insensitive to the details of the above distributions. Similar conclusions were reached earlier while considering strong collision and rotational diffusion models in the simplified manner [13,14]. One has to note that the model considered in this paper is based on the strong collision approach. In order to see a distribution of the residence time one needs distinct groups of vastly different residence times. Such situation is unlikely to occur in a homogeneous system, albeit it is quite plausible in spatially heterogeneous systems on the meso-scale, like living tissues or cells.

Experimental data on 5% ferrocene/dibutylphthalate [8] and data patterns obtained in this work are very similar.

References

[1] H. Frauenfelder, R.M. Steffen, *Alpha-, Beta- and Gamma- Ray Spectroscopy*, edited by K. Siegbahn (North Holland Publ. Corp., Amsterdam, 1968).

[2] R.M. Steffen, *Angular Correlations in Nuclear Disintegration*, ed. by H. van Krugten, B. van Nooijen (Rotterdam University Press, Wolters-Noordhoff Publishing, Groningen, The Netherlands, 1971).

[3] E. Iolin, *private communication* (1994).

[4] A.Q.R. Baron, A.I. Chumakov, S.L. Ruby, J. Arthur, G.S. Brown, G.V. Smirnov, U. van Bürck, *Phys. Rev. B* **51** (1995) 16384.

[5] J.B. Hastings, D.P. Siddons, U. van Bürck, R. Hollatz, U. Bergmann, *Phys. Rev. Lett.* **66** (1991) 770.

[6] G.V. Smirnov, *Hyperfine Interact.* **123/124** (1999) 31.

[7] U. van Bürck, *Hyperfine Interact.* **123/124** (1999) 483.

[8] I. Sergueev, U. van Bürck, A.I. Chumakov, T. Asthalter, G.V. Smirnov, H. Franz, R. Rüffer, W. Petry, in *Highlights 2002*, ed. by D. Cornuéjols and G. Admans, (ESRF, Grenoble, 2003), p. 61; *Highlights 2003*, ed. by G. Admans, (ESRF, Grenoble, 2004), p. 12.

[9] A.I. Chumakov, R. Rüffer, A.Q.R. Baron, H. Grunsteudel, H.F. Grunsteudel, V.G. Kohn, *Phys. Rev. B* **56** (1997) 10758.

[10] U. van Bürck, *private communication* (2002).

[11] M. Blume, *Phys. Rev.* **174** (1968) 351.

[12] H. Winkler, E. Gerdau, *Z. Physik* **262** (1973) 363.

[13] H. Winkler, *Z. Physik A* **276** (1976) 225.

[14] S. Dattagupta, *Hyperfine Interact.* **11** (1981) 77.

[15] K. Ruebenbauer, T. Birchall, *Hyperfine Interact.* **7** (1979) 125.

[16] U. Bengtzelius, W. Götze, A. Sjölander, *J. Phys. C* **17** (1984) 5915.

[17] H.Z. Cummins, Gen Li, Y.H. Hwang, G.Q. Shen, W.M. Du, J. Hernandez, N.J. Tao, *Z. Phys. B Condens. Matter* **103** (1997) 501.

[18] P. Boyer, in *Proceedings of XXV Zakopane School on Physics*, edited by J. Stanek and A.T. Pędziwiatr, (World Scientific Publishing Co., Singapore, 1990), p. 211.

[19] N.N. Greenwood, T.C. Gibb, *Mössbauer Spectroscopy* (Chapman and Hall Ltd, London, 1971).

[20] I. Sergueev, H. Franz, T. Asthalter, W. Petry, U. van Bürck, G.V. Smirnov, *Phys. Rev. B* **66** (2002) 184210.

[21] A. Sawaryn, L.P. Aldridge, R. Bläs, V.R. Marathe, A.X. Trautwein, *Hyperfine Interact.* **29** (1986) 1303.

[22] R. Greatrex, N.N. Greenwood, *Discuss Faraday Soc.* **47** (1969) 126.

[23] C.H.F. Peden, S.F. Parker, P.H. Barrett, R.G. Pearson, *J. Phys. Chem.* **87** (1983) 2329.

[24] G. Doppler, E. Bill, U. Gonser, F. Seel, A.X. Trautwein, *Hyperfine Interact.* **29** (1986) 1307.

[25] R. Kohlrausch, *Ann. Phys. (Leipzig)* **12** (1847) 393.

[26] E. Gerdau, R. Rüffer, R. Hollatz, J.P. Hannon, *Phys.Rev.Lett.* **57** (1986) 1141.

[27] G.V. Smirnov, V.G. Kohn, W. Petry, *Phys. Rev. B* **63** (2001) 144303.